Ecological Modelling 337 (2016) 137–148

Contents lists available at ScienceDirect

Ecological Modelling

journal homepage: www.elsevier.com/locate/ecolmodel

Modelling red coral (*Corallium rubrum*) growth in response to temperature and nutrition

Giovanni Galli[a,b,*], Lorenzo Bramanti[d], Cristina Priori[e], Sergio Rossi[f], Giovanni Santangelo[e], Georgios Tsounis[g], Cosimo Solidoro[a,c]

[a] *Dipartimento di Oceanografia, Istituto Nazionale di Oceanografia e di Geofisica Sperimentale – OGS, Borgo Grotta Gigante, Brisciki 42/c, 34010 Sgonico – Zgonik, TS, Italy*
[b] *Dipartimento Scienze della Vita, Universita Trieste, Via L. Giorgieri, 34127 Trieste, Italy*
[c] *International Centre for Theoretical Physic, ICTP, Trieste, Italy*
[d] *Laboratoire d'Ecogéochimie des Environnements Benthiques (LECOB – UMR8222), Observatoire Océanologique, Sorbonne Universités, UPMC Universités Paris 06, CNRS, 66650 Banyuls/Mer, France*
[e] *Dipartimento di Biologia, Università di Pisa, Via Volta 6, I-56126 Pisa, Italy*
[f] *Institut de Ciència i Tecnologia Ambientals (UniversitatAutònoma de Barcelona), Edifici Cn Campus UAB, Cerdanyola del Vallés, Barcelona 08193, Spain*
[g] *Leibniz Center for Tropical Marine Ecology, Fahrenheit Str. 6, D-28359 Bremen, Germany*

ARTICLE INFO

Article history:
Received 15 April 2016
Received in revised form 16 June 2016
Accepted 17 June 2016
Available online 5 July 2016

Keywords:
Bioenergetic model
Corallium rubrum
Trophic shading
Environmental niche
Biocalcification

ABSTRACT

Octocorals are marine modular organisms with high ecological and economic importance. Mediterranean Red Coral (*Corallium rubrum*), is endemic to the Mediterranean sea and neighboring Atlantic rocky shores and has been exploited for jewelry since ancient times. Despite the lack of photosynthetic symbionts (*Symbiodinium* spp.), red coral growth and survival do depend on sea water temperature, as well as on trophic conditions and other physico-chemical parameters. We developed and applied a mechanistic numerical model to describe the growth of a *C. rubrum* colony (polyps number, polyp and gametes biomass, skeletal inorganic and organic matter) as a function of food availability and seawater temperature. The model follows a bioenergetic approach and is calibrated vs available experimental observations. Model results highlight that larger colonies are more sensitive to high temperature and actual limits of the ecological niche also depend on food availability, hydrodynamic condition and coral morphology. Bioenergetic considerations also support the conclusion that, though a modular organism, red coral exhibits constrained growth, because of the competition for available food between polyps from the same colony.

1. Introduction

Corals are marine invertebrates of the phylum Cnidaria, class Anthzoa which form compact colonies made of genetically identical individual polyps. Several species, mainly belonging to the subclass Hexacorallia, form hard calcium carbonate ($CaCO_3$) skeletons which are the main constituents of the tropical coral reefs. The skeletons often present complex morphologies which give three dimensional complexity to the substratum and serve as a refuge for several species, increasing biodiversity and contributing to shape marine seascapes (Lartaud et al., 2017). In the subclass of Octocorallia, a group of species belonging to the family of Corallidae (to which the majority of the so called precious corals belong) produce hard $CaCO_3$ skeletons which are used as raw material for jewelry (Tsounis et al., 2010).

The Mediterranean red coral (*Corallium rubrum*) belongs to the family of Corallidae and is endemic to the Mediterranean sea and neighboring Atlantic rocky shores (Boavida et al., 2016; Zibrowius et al., 1984). It is commonly found in hard substrate ecosystems of prime ecological importance, such as the coralligenous assemblages (Ballesteros, 2006), on steep walls and overhangs, below 20 m deep and down to >800 m (Costantini et al., 2010; Rossi et al., 2008). Due to its economical (it is harvested for jewelry), ecological and cultural value, *C. rubrum* is considered a patrimonial species (Bramanti et al., 2011; Price and Narchi, 2015).

Besides harvesting pressure, shallow *C. rubrum* populations have been subject in recent years (1999, 2003, Garrabou et al., 2001, 2009; Bramanti et al., 2005) to mass mortalities that occurred jointly with high summer temperature anomalies. A cause and effect relationship is advocated in which mortalities are triggered by a combination of increased metabolic demands, due to high

* Corresponding author.
E-mail address: ggalli@ogs.trieste.it (G. Galli).

http://dx.doi.org/10.1016/j.ecolmodel.2016.06.010
0304-3800/

temperature, and effectively lower food ingestion, due to lower prey concentration and extended inactive feeding mode, i.e. dormant state (Rossi et al., 2006; Rossi and Tsounis, 2007; Coma et al., 2009); pathogens may also have been involved in mortality outbreaks (Martin et al., 2002). In fact *C. rubrum* is a strictly heterotrophic species and is subject to seasonal feeding constraints, with autumn/winter being more favourable than spring/summer (Rossi and Tsounis, 2007). This alternation appears to be related to the seasonal change in Mediterranean waters (Cebrian et al., 1996; Rossi and Gili, 2009), which is characterized by the development of oligotrophic waters above the thermocline during summer, whilst in winter the water column is mixed and nutrients are abundant. Food availability will thus constrain the potential recovery of damaged colonies of this and other heterotrophic organisms that depend upon seston concentration and quality to store energy and use it for their metabolic activities (Gori et al., 2013), including tissue repair. In fact Coma et al. (2009) reported that high nutritional levels can delay the appearance of necrosis in the gorgonian *P. clavata* exposed to elevated temperatures. Like other calcifying organisms, Red coral is also sensitive to acidification (decrease of pH) which might impair skeleton deposition (Bramanti et al., 2013; Cerrano et al., 2013), or increase skeleton deposition costs, or induce stress.

The interaction among different stressors is likely to be ecologically relevant for *C. rubrum*, as already observed in other Mediterranean anthozoans (Coma et al., 2009; Rodolfo-Metalpa et al., 2010). Environmental variables influence metabolic processes that are linked to organism fitness, like growth and reproduction. A bioenergetic modelling perspective can thus provide precious insight into the cause and effect mechanisms that underlie coral sensitivity to environmental variables, hence into the mechanisms of action of climate change related pressures.

Here we develop and apply a mechanistic model to describe *C. rubrum* colony growth. The model describes the growth of the average polyp and colony accretion by polyp budding and skeleton deposition, as a function of water temperature and food availability. The model is tested against available data and observed growth patterns, and the calibrated model is used to evaluate fundamental properties of *C. rubrum* potential niche with regard to food availability and temperature, as well as to quantify carbon fluxes of *C. rubrum* populations.

The only other models applied to Mediterranean coral species are (1) the matrix population model developed for *C. rubrum* by Santangelo et al. (2007, 2012) and Bramanti et al. (2009), which explores red coral demography and mass mortalities impacts on populations, (2) a metapopulation model developed by Guizen and Bramanti (2014) which takes into account the supply of larvae from distant populations, and (3) the harvesting management models (Beverton & Holt model) in García-Rodríguez and Massó, (1986), Tsounis et al. (2007). These models, although informative, assume constant colony growth rates and make no attempts to quantify polyps and colonies growth as a function of environmental variables. Also considering other coral species, the few existing models mainly focus on specific processes (and related scales). For instance the ecophysiology of biocalcification has been addressed in Hohn and Merico (2012, 2015) and Nakamura et al. (2013) by modelling the path of carbonate compounds from seawater to coral skeleton; Anthony et al. (2002) used energetic reasoning to assess the differential allocation of energy to soft tissue and skeleton across coral growth forms; Merks et al. (2003) and Chindapol et al. (2013) looked into the influence of local hydrodynamic conditions on coral morphogenesis. Habitat suitability models have also been developed on process-based grounds (Hoogenboom and Connolly, 2009) as well as based on empirical or semi-empirical reasoning (Guan et al., 2015; McCulloch et al., 2012). A review of all these applications however highlights how organism energetics remains to date an understudied topic in coral ecology. In fact, to our knowledge, the only attempt to model a whole colony, taking into account energetics and food limitation, has been carried out by Kim and Lasker (1998) to explore factors (trophic shading) that may constrain growth in colonial organisms.

From a modelling perspective, our approach relies on the coupling of a bioenergetic individual growth model, a type of model already successfully applied to a variety of organisms, including suspension feeders (Solidoro et al., 2000, 2003; Anthony et al., 2002; Kim and Lasker, 1998), with a population dynamic model and a colony resource acquisition model that accounts for competition between polyps of the same colony. A similar approach has already been applied for other (non-colonial) benthic suspension feeders (Solidoro et al., 2000, 2003) to model animal's and populations responses to different environmental conditions.

The final objective of the present paper is to simulate changes in coral calcareous mass, biomass and polyps number over time and to identify favourable and unfavorable environmental conditions by using growth as an indicator. Moreover our model allows for the interpretation of growth patterns such as skeleton accretion rings formation and the properties of modular growth, in the light of organism energetics.

2. Materials and methods

The soft tissue of a red coral colony (coenenchyme), which covers the axial skeleton, is composed of polyps (the fundamental modular units that capture, ingest and digest food particles), and of the mesoglea, an acellular collagen matrix. Polyps are potentially autonomous units, but a network of gastrovascular channels runs through the mesoglea and along the skeleton distributing resources to the entire colony (Grillo et al., 1993). Calcareous spicules are also embedded within the mesoglea. Both skeleton and spicules are composed of Magnesium-rich calcite and organic matter (OM, Grillo et al., 1993). The role of the organic portion of the skeleton is unclear and various hypotheses have been formulated, ranging from calcification control to passive incorporation (Allemand et al., 2011). The axial skeleton cross section shows annual growth rings composed of thin dark bands, alternated by thick pale bands, corresponding to slow and fast growth respectively; according to Marschal et al. (2004) thin bands, that are richer in OM, are deposited during autumn/winter, whilst thick bands (poor in OM) are deposited during spring/summer; i.e. the most of the $CaCO_3$ is deposited during the period that is regarded as trophically unfavorable.

The model is organized in two levels/scales (Fig. 1); one accounts for the growth of a single coral polyp, including organic tissues and skeletal growth, the other accounts for colony accretion by polyp budding. The state variables of the polyp growth sub-model are the energy content (in kJ) of polyp (b_P), gametes (b_G), OM (s_{OM}) and $CaCO_3$ (s_{carb}), values are converted to mass when appropriate (either g ash free dry matter, afdm, for organic tissues or g $CaCO_3$). The colony accretion sub-model state variable is the number of polyps (N_P).

2.1. Individual polyp growth model

The core structure of the polyp growth sub-model (Fig. 1) builds on the approach proposed by von Bertalanffy (1938) which described the relationship between growth and metabolism in a living organism. Accordingly, the energy gained by food intake (E_{in}) is used to support metabolic costs (basal metabolism, R_b, and energetic costs related to skeletal deposition, E_s), and to build coral polyp biomass (b_P, comprising polyp body, coenenchyme and mesoglea), gametes (b_G) and skeletal organic matter (s_{OM}).

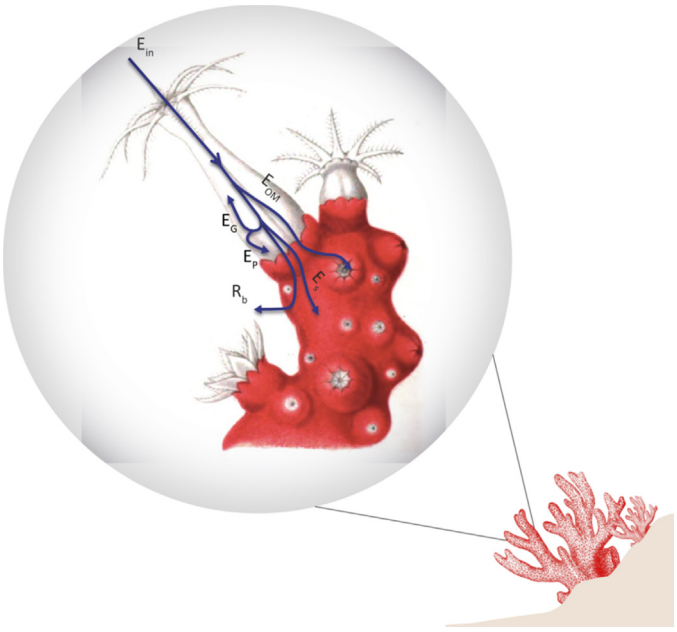

Fig. 1. Polyp growth sub-model scheme. E_{in} is energy gain by food intake, E_P, E_G, E_{OM}, and E_S are the metabolic fluxes allocated to polyp body (b_P), gametes (b_G), skeletal organic matter (s_{OM}) and $CaCO_3$ (s_{carb}) respectively, R_b is basal metabolism. Backgrowund picture from the richly illustrated Histoire Naturel by Henri de Lacaze-Duthiers.

The anabolic flux, i.e. energy inflow, is therefore defined as

$$E_{in} = C_{max} \cdot f_c(F) \cdot f_{act}(T) \cdot b_P^n \quad (1)$$

where C_{max} is the maximum energy assimilation rate, n is an allometric parameter which accounts for the fact that energy inflow is proportional to polyp surface rather than weight, $f_{act}(T)$ describes the influence of temperature, T, on polyps filtering activity (see Section 2.1.1), and $f_C(F)$ describes the influence of food concentration F in the filtered water (see Section 2.1.2).

As for metabolic processes, we defined as basal metabolism the ensemble of processes supporting vital functions in the corals, such as basal respiration. By definition these processes cannot be stopped to divert energy to other functions. Following common modelling practice and current ecophysiology theory we assume that R_b is a function of living biomass b_P, and temperature, T. It can be measured by oxygen consumption in "resting" conditions. We assume skeleton and gametes, once built, do not have maintenance costs, and therefore do not contribute to R_b.

$$R_b = R_{b,max} \cdot f_r(T) \cdot b_P^m \quad (2)$$

where $R_{b,max}$ is the maximum respiration rate, $m = 1$, and $f_r(T)$ describes the influence of temperature on respiration (see Section 2.1.1).

A formal theory of energy allocation to skeleton versus tissue growth in calcifying organisms is currently lacking. However, Anthony et al. (2002) found that basal metabolic rates are the main descriptors of energy investment into skeleton in two species of reef corals. Furthermore, specific literature indicates that *C. rubrum* skeleton is deposited continuously throughout the lifespan of the colony (Bramanti et al., 2014; Priori et al., 2013; Santangelo et al., 2007). Therefore we considered skeletal deposition as a fixed cost, similarly to basal metabolism. However, since skeletal deposition should be proportional to the colony surface, rather than to its biomass, we assumed E_s (the energy per polyp allocated to skeletogenesis) as a function of T and b_P to the power of $n = 2/3$.

$$E_s = E_{s,max} \cdot f_r(T) \cdot b_P^n \quad (3)$$

where $E_{s,max}$ is the maximal energy flux per unit surface area. This energy can then be converted to skeletal mass (s_{carb}, calcite) by using the calcification cost, e, proposed in Anthony et al., 2002:

$$\frac{ds_{carb}}{dt} = e \cdot E_s \quad (4)$$

Skeleton dissolution is not possible within the model as E_s is always positive. As already remarked, the skeleton also includes an organic fraction, which has to be formed with a different kinetic (with respect to the inorganic one) in order to generate the yearly accretion rings patterns found in *C. rubrum* (Marschal et al., 2004; Priori et al., 2013). Marschal et al. (2004) found that OM rich bands are produced during the cold season, when food is more abundant (Rossi and Gili, 2005). After such evidence we inferred that in *C. rubrum*, the acquisition of the building blocks for new OM synthesis depends on compounds supplied with food; E_{OM}, energy flux allocated to OM synthesis, is then considered to be related to feeding formulation:

$$E_{OM} = \alpha \cdot E_{in} \quad (5)$$

$$\frac{ds_{OM}}{dt} = \varepsilon \cdot \alpha \cdot E_{in} \quad (6)$$

where α is an energy partitioning coefficient (fraction of E_{in} allocated to OM formation) and e the energy to mass conversion coefficient. Our approach for describing skeleton formation is in line with the one proposed in a dynamic energy budget model (Fablet et al., 2011; Pecquerie et al., 2012) for describing the energetic costs related to deposition of calcareous otoliths in fish, there defined as a weighted sum of anabolic and catabolic fluxes.

The difference between energy intake, E_{in}, and the energetic costs, R_b, E_s, E_{OM}, defines the energy surplus (scope for growth, sfg) which is partitioned between energetic costs related to the synthesis of polyp tissues and gametogenesis, with a partitioning coefficient β. We further assume that energy is invested in reproduction only when a surplus is available ($sfg \geq 0$); In this case $E_G = (1-\beta)sfg$. In fact, Tsounis et al. (2006a) surveyed the yearly cycle of gametes development in red coral and found that gametes development was slow from September to December, coinciding with the lowest seawater carbon concentrations (a proxy for available food, Rossi and Gili, 2005).

Conversely, if permanent catabolic costs exceed the anabolic ones and sfg is negative ($sfg < 0$), then gametogenesis is stopped ($E_G = 0$) and permanent energetic costs are balanced by a reduction in polyp biomass. Accordingly, energy partitioning is described by,

$$sfg = E_{in} - R_b - E_s - E_{OM} \quad (7)$$

$$E_P = min\left(sfg, \beta \cdot sfg\right) \quad (8)$$

$$E_G = max\left(0, \left(1-\beta\right) sfg\right) \quad (9)$$

while the biomass counterpart reads,

$$\frac{db_P}{dt} = \varepsilon \cdot min\left(sfg, \beta \cdot sfg\right) \quad (10)$$

$$\frac{db_G}{dt} = \varepsilon \cdot max\left(0, \left(1-\beta\right) \cdot sfg\right) \quad (11)$$

Gametes cannot lose mass due to the absence of maintenance costs (but see Tsounis et al., 2006a). However, once a year, in August, gametes are released and b_G resets to $b_G = 0$ (Santangelo et al., 2003; Tsounis et al., 2006a).

2.1.1. Influence of temperature

Temperature affects a great variety of biological processes. We modelled the influence of temperature on polyps feeding activity, $f_{act}(T)$, based on quantifications of the fraction of open polyps in a colony (assuming that open polyps are feeding). The curve parameters are derived by fitting data from Previati et al. (2010), which

Table 1
Control functions parameter values and sources.

Control function	Parameters	Value	Units	Source
Food assimilation	k_F	0.0184	$mg_C\ cm^{-3}$	Estimated by the fitting procedure
Activity rate	T_{ah}	92014	K	Fitting from Previati et al. (2010)
	T_a	294.4	K	
Respiration rate	T_r	3170	K	Fitting from Previati et al. (2010)
	T_1	293.15	K	
	T_{rl}	−57547	K	
	T_l	287.55	K	
	T_{rh}	96549	K	
	T_h	296.75	K	
Budding rate	b_{ss}	1.68e-4	kJ	Estimated by the fitting
	b_{ah}	1.07e-5	kJ	procedure

measured polyp activity rates in *C. rubrum* over the range 14–25 °C. The function is a sigmoid shaped function ranging from 0 to 1. for parameters description and values see Table 1.

$$f_{act}(T) = 1 + exp\left(\frac{T_{ah}}{T_a} - \frac{T_a}{T}\right) \tag{12}$$

Respiration and $CaCO_3$ deposition depend upon T according to an unimodal, asymmetric curve. We used the formulation proposed in Heitzer et al. (1991) and the function has been fitted against the data on O_2 consumption rates measured for red coral over the range 14–25 °C (Previati et al., 2010). O_2 fluxes have been converted to energetic equivalents according to Gnaiger (1983). For parameters description and values see Table 1.

$$f_r(T) = \frac{\frac{T}{T_1} \cdot exp\left(\frac{T_r}{T_1} - \frac{T_r}{T}\right)}{1 + exp\left(\frac{T_{rl}}{T_l} - \frac{T_{rl}}{T}\right) + exp\left(\frac{T_{rh}}{T_h} - \frac{T_{rh}}{T}\right)} \tag{13}$$

2.1.2. Influence of trophic conditions

The actual energy intake depends on the quantity of food in the water column. Following a common modelling practice, here we assume that specific energy inflow is the product of the maximum amount of energy a polyp can process, C_{max}, and a Monod-Michaelis-Menten function on the food concentration, F, experienced by the polyps:

$$f_c(F) = \frac{F}{k_F + F} \tag{14}$$

where k_F is the semi-saturation constant. Please note that F might be different from bulk food concentration (see Section 2.4).

2.2. Polyp population dynamics

Polyp number increases by budding (asexual reproduction) and the evolution of the number of polyps in a colony over time can be described with population dynamics theory. Since other studies on *C. rubrum* (Santangelo et al., 2007, 2012; Bramanti et al., 2009; Guizen and Bramanti, 2014) also use population dynamics concepts but applied on colonies level, we clarify that here population refers to the polyps in a single colony. The evolution of polyps number, N_P, over time, is modelled as:

$$\frac{dN_P}{dt} = r_{max} \cdot f_{gem}(b_P) \cdot {N_P}^x \tag{15}$$

where r_{max} is the maximum net population growth rate (birth rate – death rate) and x is an empirical coefficient, both derived from fitting the data (polyps at age) in Santangelo et al. (2007).

No density dependence of mortality has been considered because it would have imposed growth constraints for the colony, an instance that is usually rejected for colonial species (Sebens, 1980). Instead we chose to explicitly model other factors (trophic shading, Kim and Lasker, 1998; see Section 2.4) that may contribute constraining growth.

f_{gem} [0:1] is a sigmoid shaped function of polyp mass, b_P, that describes the dependency of polyp budding rate from polyp size (see Table 1), assuming that polyps can bud only when a minimal size is attained (Sebens, 1980), it is defined as:

$$f_{gem}(b_P) = \frac{1}{1 + exp\left(\frac{b_{ss}}{b_{ah}} - \frac{b_P}{b_{ah}}\right)} \tag{16}$$

2.3. Sub-models coupling

The integration of the polyps population dynamic model and the individual polyp model allows upscaling from individual to colony level. This integration would call for a development of an age class model. However here we considered all the colony's polyps equal to an average individual and variables pertaining to the single polyp are averaged over the colony. Despite this approach should be considered a first approximation, it is useful to describe the interaction between a colony and its environment, also considering that polyps are relatively small and apparently they reach an adult size within the first years of life (Carlotta Benedetti, unpublished results), also using colony's shared resources.

The coupling of the polyp growth and polyp population dynamics implies that the average gamete and polyp biomass, b_P and b_G, change as,

$$\frac{db_P}{dt} = \frac{\partial b_P}{\partial t} - \frac{b_P}{N_P}\frac{\partial N_P}{\partial t} = \varepsilon \cdot min\left(sfg, \beta sfg\right) - \frac{b_P}{N_P} r_{max} \cdot f_{gem}(b_P) \cdot {N_P}^x \tag{17}$$

$$\frac{db_G}{dt} = \frac{\partial b_G}{\partial t} - \frac{b_G}{N_P}\frac{\partial N_P}{\partial t} = \varepsilon \cdot max\left(0, \left(1 - \beta\right) \cdot sfg\right) - \frac{b_G}{N_P} r_{max} \cdot f_{gem}(b_P) \cdot {N_P}^x \tag{18}$$

Conversely, the skeleton related fluxes, E_s and E_{OM}, join a single pool common to all polyps so that total calcite weight, S_{carb}, and total OM weight, S_{OM}, behave linearly with N_P:

$$\frac{dS_{carb}}{dt} = e \cdot N_P \cdot E_s \tag{19}$$

$$\frac{dS_{OM}}{dt} = \varepsilon \cdot N_P \cdot \alpha \cdot E_{in} \tag{20}$$

The set of differential equations is solved at monthly time steps with Runge-Kutta 4th order method. Whole colony weight (W_{Col}) at

Table 2
Model parameter values, conversion coefficients and relative sources.

Parameter	Description	Value	Units	Source
n	scaling exponent	2/3	–	–
m	scaling exponent	1	–	–
α	b_{OM} allocation coefficient	0.1482	–	Estimated by the fitting procedure
β	b_P allocation coefficient	0.7606	–	Estimated by the fitting procedure
v	flow speeds	[0.8:4]	cm h^{-1}	–
k_1	shape coefficient	0.5191	cm^2 cm^{-3}	Estimated by the fitting procedure
$R_{b,max}$	max. respiration rate	0.1107	kJ $g_{AFDM}{}^{-1}$ $month^{-1}$	Estimated by the fitting procedure
$E_{s,max}$	max. $CaCO_3$ energy allocation rate	0.0982	kJ cm^{-2} month	Estimated by the fitting procedure
C_{max}	max. assimilation rate	0.1408	kJ $month^{-1}$ cm^{-2}	Tsounis et al. (2006b), Picciano and Ferrier-Pagès (2007)
r_{max}	max. gemmation rate	2.664	y^{-1}	Fitted from Santangelo et al. (2007)
x	allometric scaling exponent	0.563	–	Fitted from Santangelo et al. (2007)
–	conversion coefficient	45.7	kJ $g_C{}^{-1}$	Brey (2001) and refs therein
–	molecular weight of O_2	3.2e4	mg mol^{-1}	–
–	oxyenthalpic equivalent	473	kJ $mol_{O2}{}^{-1}$	Gnaiger (1983)
e	biomass energy content	27.203	kJ $g_{AFDM}{}^{-1}$	Brey (2001) and refs therein
e	$CaCO_3$ metabolic cost	0.152	kJ $g_{CaCO3}{}^{-1}$	Anthony et al. (2002)

time t results from the sum of the various components once proper conversion coefficients (see Table 2) have been applied:

$$W_{Col}(t) = S_{carb}(t) + S_{OM}(t) + N_P(t) \cdot (b_P(t) + b_G(t)) \quad (21)$$

2.4. *Trophic shading and polyps* intra-colonial *polyp competition*

The actual food concentration experienced by a polyp might differ from the bulk concentration, because of competition among polyps of the same colony. In fact, in colonial organisms inner polyps might process water that has been already partially filtered by outer polyps (Kim and Lasker, 1998). This effect has been parameterized as following. Let Q be the water flow through a colony and F_b the bulk food concentration. Then the variation of the mass of food, M, in a control volume V around a colony of surface area S is:

$$\frac{dM}{dt} = Q \cdot (F_b - F) - C_{max} \cdot f_{act}(T) \cdot f_c(F) \cdot S \quad (22)$$

where F is food concentration in the control volume and the surface S is dimensionally related to $N_P \cdot {b_P}^{2/3}$. Assuming that stationary conditions are reached rather quickly, we can equate the right hand side of the equation to zero and solve for F, which gives:

$$F^2 + F \cdot (k_F - F_b + \frac{C_{max} \cdot f_{act}(T) \cdot S}{Q}) - k_F \cdot F_b = 0 \quad (23)$$

that admits just one positive solution:

$$F = \frac{-(k_F - F_b + \boldsymbol{G}) + \sqrt{(k_F - F_b + \boldsymbol{G})^2 + 4 k_F F_b}}{2} \quad (24)$$

where

$$G = \frac{C_{max} \cdot f_{act}(T) \cdot S}{Q} \quad (25)$$

is the ratio between maximal colony assimilation rate at a given temperature and water flow per unit area.

This way, if the colony processing capability is much lower than water supply, G is small and F roughly equal to F_b, whereas in the opposite case, F is greatly reduced.

Now let the control volume V be cubic so that the area of a face is $A_S = V^{2/3}$, and let the flow be oriented normally to two faces so that,

$$Q = v \cdot A_S = v \cdot V^{2/3} \quad (26)$$

where v is flow speed. If we assume that a branching coral grows according to a space filling pattern (Kruszyński et al., 2007) so that the colony surface area S per unit of control volume V is roughly constant,

$$\frac{S}{V} = k_1 \quad (27)$$

we can express G also as a function of water velocity and coral surface area:

$$G = \frac{C_{max} \cdot f_{act}\ T \cdot S}{Q} = \frac{C_{max} \cdot f_{act}\ T \cdot S^{1/3}}{v \cdot k_1^{-2/3}} \quad (28)$$

2.5. *Boundary conditions and initialization*

The baseline simulation is forced with monthly average water temperature, recorded by the meteorological station of l'Estartit, Catalan coast, over the period 1973–1997, (Cebrian et al., 1996). Among the sampled depths the 35 m record was used in most of the simulations. Simulations are also forced with monthly average total Carbon, C_{tot}, measured at 20 m depth and right above the benthic community, considered as a proxy for available food (Medes islands, Catalan coast, 1997–1998, Rossi and Gili, 2005) and converted to energy according to Brey (2001). Few data are available about near-bottom seston in the Mediterranean. Rossi and Gili (2005) highlight how values can be substantially higher than in open waters and detected a pronounced seasonality (that is typical in open waters) only for chlorophyll records, supporting that the 20 m C_{tot} data we use to constrain the model may be representative of carbon load also in deeper waters where *C. rubrum* is most commonly found. This assumption however is not crucial for model results as it will affect just the magnitude of seasonal variations in metabolic rates, and not the general model behavior.

The initial value for b_P and N_P are set to 10^{-5} kJ and one polyp respectively whilst S_{carb}, S_{OM} and b_G initial values are set to zero. The simulation begins in August, when spawning usually takes place (Tsounis et al., 2006a).

2.6. *Model calibration*

Model calibration is performed on datasets where the three variables polyps number, colony weight and age were measured in red coral populations. The sets are from Santangelo et al. (2007) (13 data points averaged from a larger sample of 1802 colonies, polyps and age data, Fig 3a, blue dots) and Priori et al. (2013) ($n = 69$ colonies, polyps, dry weight and age data, Fig. 2a, b and Fig. 3a, b, red dots).

The two sets of accretion data reflect a number of red coral growth features. Santangelo et al. (2007) data consist of a large sam-

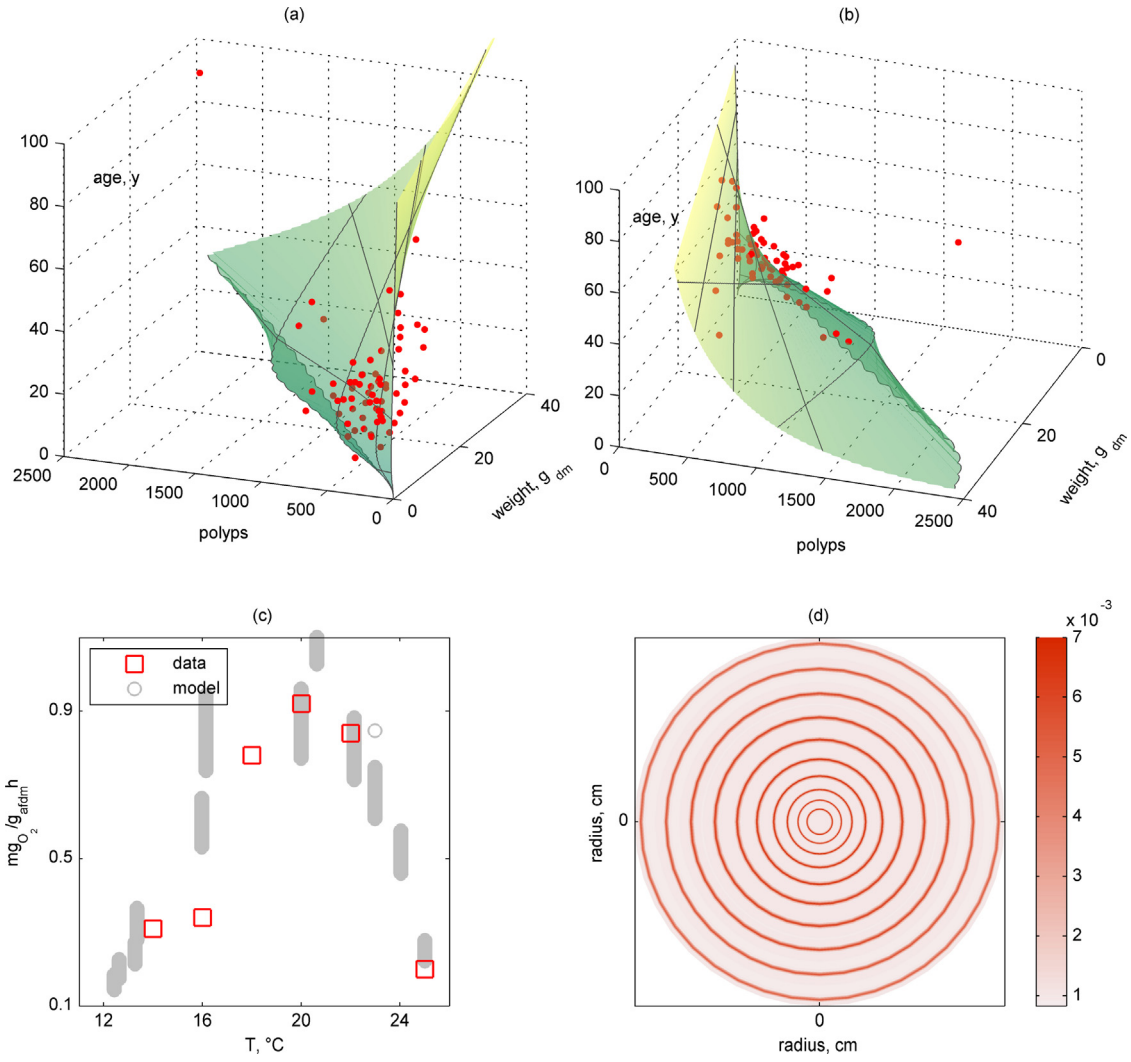

Fig. 2. Model results and fitting. (a) and (b): two views of the colony growth surface, model results (green surface) and experimental data (red dots, Priori et al., 2013). (c): Total respiration, grey circles: model results, red squares: data from Previati et al., 2010; results obtained by forcing the model with an artificial temperature time series that covers all the range tested in Previati et al., 2010. (d): Representation of skeletal banding as a stylized branch cross section, colorbar units are OM weight over total skeleton weight (S_{OM} + S_{carb}). (For interpretation of the references to color in this figure legend, the reader is referred to the web version of this article.)

ple from a single population and show a regular and exponential growth of the colony (via polyps budding) during at least the first decade of a colony's life. On the other hand Priori et al. (2013) data from different populations cover a wider set of ages and display no clear correlation between age and polyp number nor age and weight: growth features seem to be highly dependent on life history traits, possibly microclimatic conditions and/or partial mortality events. If the two sets are compared, it can be inferred that the initial phase of exponential growth must cease as colonies grow bigger, possibly due to competition for food and/or space between polyps of the same colony (Kim and Lasker, 1998) and/or with neighboring organisms, including conspecifics.

Given the variability of the calibration sets, no single growth curve can satisfactorily approximate all the experimental data. Thus we assumed they represent the time trajectories of different colonies that grew in different environmental conditions (also considering microenvironment variability). The scope of parameterization was thus to fit the data against a set of model runs (that generate a growth surface in N_P, W_{Col}, time space), obtained by changing the flow speed v in Eq. (27), This is equivalent to setting lower F_b values or decreasing polyps activity, or any other combination of factors that change the number $\boldsymbol{G}$. The hypothesis we tested with this approach is that local trophic conditions alone are capable of producing most of the observed variability in growth.

Model fitting is performed on eight selected uncertain parameters (α, β, k_F, $R_{b,max}$, $E_{s,max}$, b_{ss}, b_{ah}, k_1, see Tables 1 and 2) with a Monte Carlo simulation. The algorithm minimizes of the sum of squared distances between each experimental point in N_P, W_{Col}, time space and the generated growth surface. The distances are computed on standardized data coordinates as units on N_P, W_{Col} and time axes are different. Both simulated and experimental data are standardized with mean and standard deviation of the experimental set to maintain the ratio between the two sets. Also The sum of the R_b and E_s terms is converted to oxygen consumption and confronted with the respiration rates measured in Previati et al. (2010). The sum of squared distance between measured and simulated respiration is also minimized by the fitting procedure.

2.7. C. rubrum *feeding intensity*

To estimate the feeding intensity of an average red coral population we used data on age classes areal distribution from Santangelo

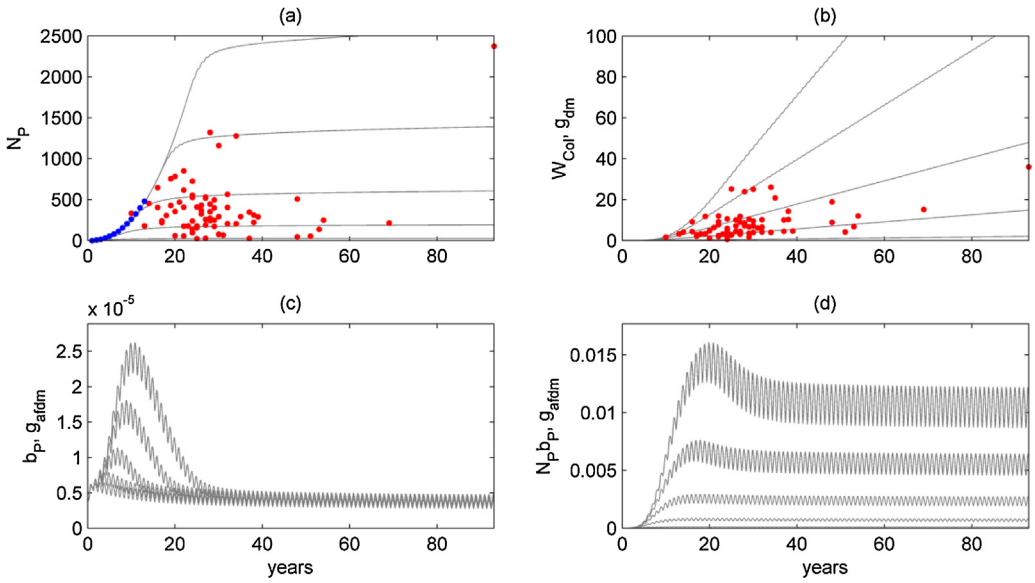

Fig. 3. Simulation results (multiple runs with varied v). Red dots: experimental data from Priori et al., 2013; blue dots: data from Santangelo et al., 2003. (a): Polyps number. (b): Colony weight (skeleton and organic tissues). (c): Average polyp weight. (d): Coenenchyme biomass (= $N_P b_P$). (For interpretation of the references to color in this figure legend, the reader is referred to the web version of this article.)

et al. (2007) and the carbon intake rates per colony calculated by the model for the same age classes.

2.8. Niche estimation

The calibrated model is also used to estimate the fundamental niche of red coral with respect to available food and temperature. We use the variation of coenenchyme biomass ($b_P \cdot N_P$) over a time period $t - t_0$, DB_{coen}, as a proxy for organism-level fitness (Hoogenboom and Connolly, 2009; Maltby, 1999).

$$DB_{coen} = \frac{N_P\ t\ \cdot b_P\ t\ - N_P\ t_0\ \cdot b_P\ t_0}{N_P\ t_0\ \cdot b_P\ t_0} \tag{29}$$

DB_{coen} is computed over a range of (constant) temperatures and bulk food concentrations and for different colony sizes, defined by initializing the model with different $b_P(t_0)$, $N_P(t_0)$ pairs from a baseline simulation. DB_{coen} is computed over 10 years as we are looking for long term effects. The resulting zero DB_{coen} isoclines are indicative of fundamental niche borders in T, F_b space for the specified size class at a fixed flow speed. The model was coded in MatLab and the code is available from the authors upon request.

3. Results

3.1. Fitting to experimental datasets

The model generates growth trajectories (a growth surface in N_P, W_{Col}, time space, Fig. 2a, b and Fig. 3a, b) that approximate most of the calibration data points just by varying flow speed (or equivalently $\boldsymbol{G}$). This result is in line with the conjecture, suggested by calibration sets and expert's opinions, that colony's accretion depends strongly on the local environment and points towards hydrodynamic and trophic conditions as major factors affecting colony growth.

Polyp population dynamics (Fig 3a) follow an initial phase of exponential growth that closely matches Santangelo et al. (2007) data for high flow speeds. This exponential growth is dampened as N_P increases, as it can be also inferred from the experimental data. This trend is due to decreasing b_P with age, negatively affecting the f_{gem} function that controls budding rate.

Whole colony mass is mostly composed of $CaCO_3$. New skeleton is produced throughout the lifetime, the simulated growth curves (Fig. 3b) are initially exponential but approach linearity as b_P decreases with age.

The simulated respiration rates (Fig. 2c) also display good agreement with Previati et al. (2010) data.

3.2. Features of live tissue growth

The simulated live tissue (b_P) shows a marked seasonal cycle (Fig. 3c, d): positive growth lasts approximately from January to June, when energy gain exceeds losses, and is followed by a negative growth phase from approximately July to December. This effect depends strongly on temperature regimes affecting both the gain and loss terms and on seasonality of food supply. In fact the biomass seasonal cycle is more marked when the model is forced with temperature records from relatively shallow (up to 35 m) waters, that are characterized by wide temperature variations; Biomass oscillations are instead dampened if the less variable deep waters records (50–80 m) are used to force temperature (not shown). The same seasonality is present also in skeletal organic matter, S_{OM} (Fig 2d), and gametes, b_G, dynamics.

The single polyp (Fig. 3c) and gametes (not shown) simulated growth trajectories are characterized by a maximum within the first decade of life, followed by an exponential decay with a horizontal asymptote reached after about 20–30 years. The position of the maximum varies depending on external conditions (feeding, temperature). Two major processes contribute to this pattern. One concerns the trophic shading effects that limit food intake per polyp for high polyp number, resulting in decreasing E_P and E_G after the maximum; the other concerns f_{gem} limiting polyp budding at low E_p, thus slowing down biomass decrease.

Coenenchyme and gamete biomass per colony (= $N_P \cdot b_P$ and $N_P \cdot b_G$ respectively, Fig 3d, gamete dynamics not shown) are characterized by determinate growth. Decreasing growth rates with colony size are mostly due to polyps population dynamics via f_{gem}

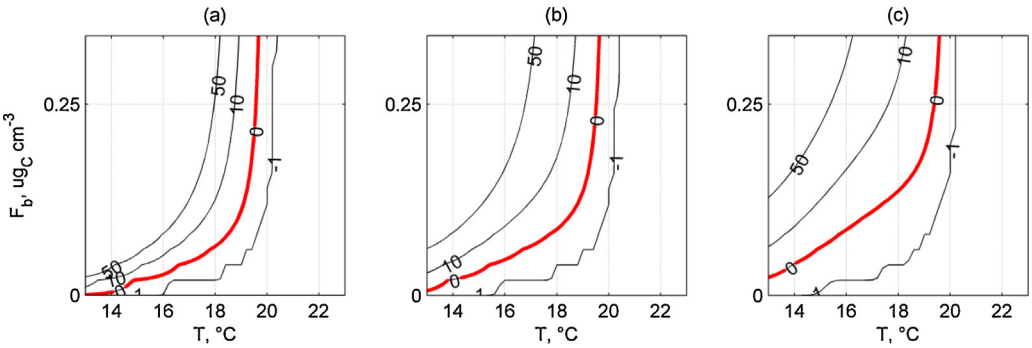

Fig. 4. Suitability diagrams computed as coenenchyme biomass change (DB_{coen}) over 10 y simulation. DB_{coen} values are plotted against different temperatures and bulk food concentrations, at fixed flow speed ($v = 3.03\,cm\,h^{-1}$) and for different colony sizes. (a): small colony: 11 polyps, 0.1e-4 g_{afdm}/polyp, (b): medium colony: 70 polyps, 0.2e-4 g_{afdm}/polyp, (c): large colony: 847 polyps, 0.05e-4 g_{afdm}/polyp). The zero isoclines (in red) represent the distribution limits for the specified colony size. Other isoclines are merely indicative of trends as their position depends on simulation time. (For interpretation of the references to color in this figure legend, the reader is referred to the web version of this article.)

that limits new polyps production at low b_p and is thus closely tied to the b_P evolution.

3.3. Features of skeleton growth

$CaCO_3$ seasonal deposition (Fig. 2d) follows a reverse pattern with respect to organic tissues, including S_{OM}. Most of the skeleton is deposited during the warmer period, when the E_s term is maximum due to high temperatures. And whilst live tissue growth slows down as a result of the balance between energetic intake and losses, new skeleton is produced throughout the lifetime.

The model simulates the differential incorporation of $CaCO_3$ and organic matter in the coral skeleton described in Marschal et al. (2004). During cold months environmental conditions are favourable for tissue growth, hence much organic matter is deposited whilst $CaCO_3$ flux is low due to low respiration rates; since organic matter flux is larger than $CaCO_3$ flux, this results in the deposition of low quantity of material (thin band), relatively rich in organic matter. On the contrary during warm months trophic conditions are poor and a low quantity of organic matter is produced whilst $CaCO_3$ flux is high due to high respiration rates, resulting in the deposition of a thick band that is poor in organic matter. The average proportion of S_{OM} to S_{carb} in the skeleton is however underestimated with respect to the values reported in Allemand and Bénazet-Tambutté (1996) (0.012–0.017 on weight basis).

3.4. Niche estimation

As far as fundamental niche estimation is concerned (Fig. 4) our model predicts that smaller colonies have potential for positive growth over a wider region in F_b-T space than large colonies do, especially at low food concentrations. This means a large colony is more demanding in terms of seawater food concentration to sustain its size when temperatures are high, whilst small colonies can thrive over a broader range of conditions. In Fig. 4 the zero isocline ($DB_{coen} = 0$) is indicative of the niche borders for different size classes and, unlike the rest of the isoclines, its position is not affected by the time window over which DB_{coen} is computed.

3.5. Feeding intensity

The estimated feeding intensity of a typical red coral shallow population composed mainly of relatively young colonies, such as the one sampled in Santangelo et al. (2007) is of 0.17 $mg_C\,m^{-2}\,d^{-1}$ which is within the range estimated in Tsounis et al. (2006b) (0.15–1.5 $mg_C\,m^{-2}\,d^{-1}$).

4. Discussion

In the present work we developed a colony growth model to better understand the influence of temperature, food concentration and hydrodynamic regime on the growth of *C. rubrum* colonies and to investigate the challenges that this and other related organisms may face in front of climate change. This model may also serve to exemplify how heterotrophic colonial organisms may be modelled in a bioenergetic framework. Among bioenergetic modelling frameworks our model may fall in the list of those sometimes referred to as Scope for Growth (Ursin, 1967). This class of models is characterized by lower complexity as opposed to the more detailed approach of Dynamic Energy Budget theory (DEB, Kooijman, 2010). DEB theory enjoys considerable regard and has been intensively explored in recent years; it is characterized by a fine level of detail (e.g. storage and delayed use of energy, maturity maintenance costs, costs related to the growth process), but also larger sets of data are needed for reliable parameterization. In our case the peculiarities of the test species (clonality, biocalcification) represent additional complexity whilst on the other hand data availability constraints call for a compromise between realism and tractability. Our model represents an intermediate complexity solution that offers the advantage of being easier to parameterize with the available data, while also performing possibly equally well as a DEB model (Filgueira et al., 2011).

We produced simulations that match measured growth patterns as well as multiple observed features of *C. rubrum* colony growth and of its interactions with the environment. Furthermore the model allows for the interpretation of those features in the light of organism energetics. The originality of the approach lies in the choice of modelling *C. rubrum* as a colony of individuals, where single polyp and colony dynamics influence each other and the outcomes emerge from the interaction of the two.

4.1. C. rubrum *niche*

By using growth potential as a proxy for organism fitness, we derived an estimation of *C. rubrum* requirements, in terms of average water temperature and food concentration, to sustain positive growth, i.e. its fundamental niche in temperature-food space.

We found the limits of *C. rubrum* distribution (as identified by the zero-growth isoclines in Fig. 4) to be dependent on colony size: large colonies are more demanding than small ones with regard to temperature and food availability. These findings may help explain the observations made by Garrabou et al. (2001) that medium and large-sized colonies of *C. rubrum* from shallow waters suffered

higher mortality incidence than small ones during a mass mortality event that occurred jointly with a positive temperature anomaly and summery food shortage.

Our results also have implications regarding the size distribution of *C. rubrum* colonies: as noted by many, shallow populations are usually composed of dense patches of small individuals while larger colonies are found at higher depths at lower densities (Santangelo and Bramanti, 2010; Garrabou et al., 2001; 400–600 colonies/m^2 and Tsounis et al., 2006a; 150–250 colonies/m^2 in shallow waters, compared to Priori et al., 2013 and Rossi et al., 2008; 10–50 colonies/m^2 in deep waters); this appears to be primarily a consequence of overharvesting of the shallow, easily accessible populations that selectively removes the large specimens (Cau et al., 2016; Santangelo and Bramanti, 2010; Tsounis et al., 2007). Our findings indicate that large colonies are also more likely to undergo negative growth in shallow waters, where they experience both high temperatures and food shortage at the same time during late summer, and are thus less likely to be found near the upper distribution limits of *C. rubrum*. In deeper waters larger colonies may have less constraints due to both quite stable temperature (12–17 °C, Fiorillo et al., 2013) and food input (Gori et al., 2012). A similar size gradient with small individuals dominating the upper distribution limit has been reported by Sebens (2002) concerning the distribution of sea anemones in relation to environmental parameters. If this temperature effect on size distribution is superimposed on the harvesting effect, the occurrence of large colonies could be further limited to deeper waters as mean sea temperatures increase. Increasing trend of harmful heat waves events would also increase this risk.

In contrast, Hoogenboom and Connolly (2009) found that the niche size of reef corals in flow-light space, as calculated with a process-based model, was positively related to colony size. The Hoogenboom and Connolly (2009) model uses daily integrated energy acquisition (photosynthesis) as a proxy for fitness, but since organism energy budget is not computed, it is not possible to assess if such a rate is enough to sustain positive growth across different colony sizes; also size dependence of photosynthesis rate is calculated solely according to mass exchange kinetics from fluid mechanics theory, thus neglecting possible trophic shading effects, which the authors acknowledge.

4.2. Seasonality, trophic shading and constraints to growth

The simulated live tissue biomass displays seasonal cycles of positive and negative growth which are strongly dependent on temperature regimes and are thus more marked when the model is forced with shallow waters thermal records. Similarly Rossi and Tsounis (2007) and Tsounis et al. (2006b) uncovered a seasonality in energy storage molecules concentrations (proteins, carbohydrates, lipids) and gametes development in shallow (16–18 m) red coral colonies, whilst in deeper populations (45 m) seasonality was detectable only for protein concentration and gametes development. The same seasonal pattern is also typical of other Mediterranean benthic invertebrates, both colonial (Coma et al., 1998; Coppari et al., 2016; Gori et al., 2012) and non-colonial (Coppari et al., 2014) and appears to be related to NW Mediterranean climate seasonality. In fact, so far as near bottom seston seasonality is considered, it has been demonstrated that suspension feeders from NW Mediterranean store in spring the energy they need for the rest of the year (Coppari et al., 2014, 2016). This seasonal pattern may thus affect also other organisms that depend on the seasonal seston fluctuations (Rossi and Gili, 2005).

According to our simulations, the whole colony live tissue biomass (Fig. 3d) has a determinate growth, i.e. there exists an upper limit to colony size. The point is not trivial, in fact it is generally assumed that colony resource acquisition is simply a linear function of the number of modules, colonies would thus be free from the constraints that limit the size of the single modules and could grow indefinitely, by simply adding new modules (Sebens, 1987). It is presently unclear whether colonial organisms have a determinate or indeterminate growth, but data on *C. rubrum* size and age classes distribution (Priori et al., 2013) show that, at least in *C. rubrum*, growth slows down in older (and bigger) colonies.

In our model colony size limits, instead of being imposed with allometric constraints (as in Kim and Lasker, 1998), emerge as a consequence of trophic shading, i.e. the competition for a limited resource (food) between the polyps of the same colony. This is in line with the argument found in Kim and Lasker (1998) that density dependent effects on resource capture rates, analogous to self-shading in trees, may effectively limit maximal size in modular species that would otherwise exhibit indeterminate (exponential) growth. We also found that this result is not generally extendable to any colonial organism as the assumption in Eq. (27) does not apply to every growth shape (e.g. it does not apply for a sphere), and will result in uptake rates that scale linearly with modules number, hence in unconstrained growth, for massive growth forms. Our implementation provides thus a theoretical background for a conjecture (the existence and relevance of trophic shading phenomena and their implications for growth determinacy or indeterminacy in colonial and modular organisms) that to date rests on anecdotal evidence and speculative arguments.

The model predicts the average polyp biomass to decrease with age once a maximal value is reached early in life as a result of competition between polyps. In support of our findings an inverse relationship between the two quantities have been described by Porter (1976) for Caribbean corals; Kim and Lasker (1998) proposed that such negative correlation can result from the additive effects of module size and colony size on self-shading and thus the ability of a colony to capture resources.

4.3. Skeletal growth

Despite current research increasingly shedding light on the processes involved in biomineralization, the present understanding of the mechanisms of integration between major metabolic processes and coral skeleton formation remains weak (Allemand et al., 2011). In the present work we addressed this issue by relating skeleton formation to coral energy budget with the fraction of metabolism devoted to calcite deposition and the (proposed) energetic cost required per unit of $CaCO_3$ deposited. This modelling choice has been proven effective in reproducing observed patterns. At the same time it remains parsimonious with respect to assumptions and parameters requirements, relatively to the finer-scale modelling approaches to biocalcification found in Hohn and Merico (2012, 2015) and Nakamura et al. (2013). Our approach aims at modelling the growth of calcified structures at whole organism level and can be considered as a simplification of such models.

Skeletal growth modelling choices are similar to those in Fablet et al. (2011) and Pecquerie et al. (2012). In such works, and in the present work as well, the temperature dependences affecting skeletal deposition are those affecting the relevant physiological rates and temperature effects on $CaCO_3$ precipitation kinetics are neglected. The question whether inorganic deposition kinetics that are observed in seawater are also valid in the gel-like extracellular calcifying medium is currently debated (Allemand et al., 2011). However, the observation that the most abundant deposition of $CaCO_3$ (the thick bands in the skeleton) occurs during the warmest months, is easily linked to inorganic $CaCO_3$ precipitation being favoured at higher temperatures (e.g. McCulloch et al., 2012). Our study suggests a complementary mechanism for the observed

seasonality in $CaCO_3$ deposition. Also the underestimation of the proportion of OM to $CaCO_3$ in the skeleton, which depends on the parameterization of E_s and E_{OM}, may suggest that the mechanism of OM incorporation is not entirely passive, as implemented here, in fact many studies (see Tambutté et al., 2007 for a review) suggest that OM plays a structural role in skeleton formation, so that the two fractions could obey some kind of stoichiometric law.

Whilst live tissue growth slows down with age, our results point at indeterminate skeletal growth, seemingly leading to the unrealistic condition of the coenosarc becoming progressively thinner over a colony's life. This could have been addressed by decreasing the energy allocation to skeleton in function of colony size, this solution however seemed too much of an artefact. Indeed constant basal diameter growth rates have been observed in *C. rubrum* by Santangelo et al. (2007), Priori et al. (2013), Bramanti et al. (2014) over wide sets of ages, and Bramanti et al. (2014) found the surface area increment in *C. rubrum* skeleton cross sections to be well fitted by a linear equation, indicating constant increment along colony life span. Other explanations are possible: (1) The coenosarc thinning, despite occurring, is negligible over a colony's lifespan. (2) Additional cortex mineralization compensates for coenosarc thinning; in fact Weinbauer et al. (2000) reported levels of cortex mineralization as high as $76 \pm 6\%$ on weight basis for red coral.

Our model agrees with observations by Marschal et al. (2004) in placing maximal $CaCO_3$ deposition during the warm months, when biomass, on the contrary, displays negative growth. The same seasonal pattern has been described by Rodolfo-Metalpa et al. (2010) in the Mediterranean hexacoral *Cladocora Caespitosa*. Although seemingly paradoxical, weak coupling between growth of tissue and calcified structures is known to occur in bivalves (Hilbish, 1986), fish otoliths (Neat et al., 2008) and has been reported for scleractinian corals by Anthony et al. (2002) who measured positive skeletal growth rates even in experimental treatments where tissue growth was negative.

Even though $CaCO_3$ deposition is regarded as a process of low energetic cost (Anthony et al., 2002; McCulloch et al., 2012; Palmer, 1992), it clearly entails some metabolic cost for the coral. We suggest that skeletogenesis is sustained during energy shortage by the reserves accumulated during the previous favourable period.

5. Conclusions

In this work we presented and tested a bioenergetic approach for modelling the growth of the Mediterranean octocoral *C. rubrum* and its relation with temperature, nutrition and hydrodynamics. We also show how such kind of model can be useful in providing insight into a species ecology. According to our results environmental niche breadth for *C. rubrum* is (also) a function of colony size, thus the largest specimen are predicted to be more sensitive to warming. We also provide a formalization for trophic shading processes and conclude that, depending on colony morphology, the competition among modules may effectively impose limits to growth in colonial animals. Moreover some of the issues addressed by our model, such as clonality, biocalcification and trophic shading, are seldom explored in bioenergetic modelling practice; this work may thus serve as a basis for developing models for related species.

Aknowledgements

We'd like to thank Valentina Mosetti (OGS) for the model scheme in Fig. 1 and Carlotta Benedetti (University of Pisa) for useful discussion on polyp development.

References

Allemand, D., Bénazet-Tambutté, S., 1996. Dynamics of calcification in the mediterranean red coral, Corallium rubrum (Linnaeus) (Cnidaria, Octocorallia). J. Exp. Zool. 276, 270–278, http://dx.doi.org/10.1002/(SICI)1097-010X(19961101)276:4<270::AID-JEZ4>3.0.CO;2-L.

Allemand, D., Tambutté, É., Zoccola, D., Tambutté, S., 2011. Coral calcification, cells to reefs. In: Dubinsky, Z., Stambler, N. (Eds.), Coral Reefs: An Ecosystem in Transition. Springer, Netherlands, Dordrecht, pp. 119–150, http://dx.doi.org/10.1007/978-94-007-0114-4_9.

Anthony, K.R.N., Connolly, S.R., Willis, B.L., 2002. Comparative analysis of energy allocation to tissue and skeletal growth in corals. Limnol. Oceanogr. 47, 1417–1429, http://dx.doi.org/10.4319/lo.2002.47.5.1417.

Ballesteros, E., 2006. Mediterranean coralligenous assemblages: a synthesis of present knowledge. Oceanogr. Mar. Biol. Annu. Rev. 44, 123–195.

Boavida, J., Paulo, D., Aurelle, D., Arnaud-Haond, S., Marschal, C., Reed, J., Gonçalves, J.M.S., Serrao, E.A., 2016. A well-kept treasure at depth: precious red coral rediscovered in Atlantic deep coral gardens (SW Portugal) after 300 years. PLoS One 11, e0147228, http://dx.doi.org/10.1371/journal.pone.0147228.

Bramanti, L., Magagnini, G., De Maio, L., Santangelo, G., 2005. Recruitment, early survival and growth of the Mediterranean red coral Corallium rubrum (L. 1758), a 4-year study. J. Exp. Mar. Bio. Ecol. 314, 69–78, http://dx.doi.org/10.1016/j.jembe.2004.08.029.

Bramanti, L., Iannelli, M., Santangelo, G., 2009. Mathematical modelling for conservation and management of gorgonians corals: youngs and olds, could they coexist? Ecol. Model. 220, 2851–2856, http://dx.doi.org/10.1016/j.ecolmodel.2009.01.031.

Bramanti, L., Vielmini, I., Rosii, S., Stolfa, S., Santangelo, G., 2011. Involvement of recreational scuba divers in emblematic species monitoring: the case of Mediterranean red coral (Corallium rubrum). J. Nat. Conserv. 19, 312–318, http://dx.doi.org/10.1016/j.jnc.2011.05.004.

Bramanti, L., Movilla, J., Guron, M., Calvo, E., Gori, A., Dominguez-Carrió, C., Grinyó, J., Lopez-Sanz, A., Martinez-Quintana, A., Pelejero, C., Ziveri, P., Rossi, S., 2013. Detrimental effects of ocean acidification on the economically important Mediterranean red coral (Corallium rubrum). Global Change Biol. 19, 1897–1908, http://dx.doi.org/10.1111/gcb.12171.

Bramanti, L., Vielmini, I., Rossi, S., Tsounis, G., Iannelli, M., Cattaneo-Vietti, R., Priori, C., Santangelo, G., 2014. Demographic parameters of two populations of red coral (Corallium rubrum L. 1758) in the North Western Mediterranean. Mar. Biol. 161, 1015–1026, http://dx.doi.org/10.1007/s00227-013-2383-5.

Brey, T., 2001. Population dynamics in benthic invertebrates. A virtual handbook. Version 01.2 [WWW Document]. URL http://www.thomas-brey.de/science/virtualhandbook.

Cau, A., Bramanti, L., Cannas, R., Follesa, M.C., Angiolillo, M., Canese, S., Bo, M., Cuccu, D., Guizien, K., 2016. Habitat constraints and self-thinning shape Mediterranean red coral deep population structure: implications for conservation practice. Sci. Rep. 6, 23322, http://dx.doi.org/10.1038/srep23322.

Cebrian, J., Duarte, C.M., Pascual, J., 1996. Marine climate on th costa brava (northwest Mediterranean) littoral. Publ. Espec. Inst. Esp. Oceanogr. 22, 9–21.

Cerrano, C., Cardini, U., Bianchelli, S., Corinaldesi, C., Pusceddu, A., Danovaro, R., 2013. Red coral extinction risk enhanced by ocean acidification. Sci. Rep. 3, 1457, http://dx.doi.org/10.1038/srep01457.

Chindapol, N., Kaandorp, J.A., Cronemberger, C., Mass, T., Genin, A., 2013. Modelling growth and form of the scleractinian coral Pocillopora verrucosa and the influence of hydrodynamics. PLoS Comput. Biol. 9, http://dx.doi.org/10.1371/journal.pcbi.1002849.

Coma, R., Ribes, M., Gili, J.M., Zabala, M., 1998. An energetic approach to the study of life-history traits of two modular colonial benthic invertebrates. Mar. Ecol. Prog. Ser. 162, 89–103, http://dx.doi.org/10.3354/meps162089.

Coma, R., Ribes, M., Serrano, E., Jiménez, E., Salat, J., Pascual, J., 2009. Global warming-enhanced stratification and mass mortality events in the Mediterranean. Proc. Natl. Acad. Sci. U. S. A. 106, 6176–6181, http://dx.doi.org/10.1073/pnas.0805801106.

Coppari, M., Gori, A., Rossi, S., 2014. Size, spatial, and bathymetrical distribution of the ascidian Halocynthia papillosa in Mediterranean coastal bottoms: benthic-pelagic coupling implications. Mar. Biol. 161, 2079–2095, http://dx.doi.org/10.1007/s00227-014-2488-5.

Coppari, M., Gori, A., Viladrich, N., Saponari, L., Canepa, A., Grinyó, J., Olariaga, A., Rossi, S., 2016. The role of Mediterranean sponges in benthic–pelagic coupling processes: Aplysina aerophoba and Axinella polypoides case studies. J. Exp. Mar. Bio. Ecol. 477, 57–68, http://dx.doi.org/10.1016/j.jembe.2016.01.004.

Costantini, F., Taviani, M., Remia, A., Pintus, E., Schembri, P.J., Abbiati, M., 2010. Deep-water corallium rubrum (L., 1758) from the Mediterranean Sea: preliminary genetic characterisation. Mar. Ecol. 31, 261–269, http://dx.doi.org/10.1111/j.1439-0485.2009.00333.x.

Fablet, R., Pecquerie, L., de Pontual, H., Høie, H., Millner, R., Mosegaard, H., Kooijman, S.A.L.M., 2011. Shedding light on fish otolith biomineralization using a bioenergetic approach. PLoS One 6, http://dx.doi.org/10.1371/journal.pone.0027055.

Filgueira, R., Rosland, R., Grant, J., 2011. A comparison of scope for growth (SFG) and dynamic energy budget (DEB) models applied to the blue mussel (Mytilus edulis). J. Sea Res. 66, 403–410, http://dx.doi.org/10.1016/j.seares.2011.04.006.

Fiorillo, I., Rossi, S., Alva, V., Gili, J.M., López-González, P.J., 2013. Seasonal cycle of sexual reproduction of the Mediterranean soft coral Alcyonium acaule (Anthozoa, Octocorallia). Mar. Biol. 160, 719–728, http://dx.doi.org/10.1007/s00227-012-2126-z.

García-Rodríguez, M., Massó, C., 1986. Modelo de explotacioín por buceo del coral rojo (Corallium rubrum L.) del Mediterráneo. Bol. Inst. Esp. Oceanogr. 3, 75–82.
Garrabou, J., Pérez, T., Sartoretto, S., Harmelin, J.G., 2001. Mass mortality event in red coral Corallium rubrum populations in the Provence region (France, NW Mediterranean). Mar. Ecol. Prog. Ser. 217, 263–272, http://dx.doi.org/10.3354/meps217263.
Garrabou, J., Coma, R., Bensoussan, N., Bally, M., Chevaldonné, P., Cigliano, M., Diaz, D., Harmelin, J.G., Gambi, M.C., Kersting, D.K., Ledoux, J.B., Lejeusne, C., Linares, C., Marschal, C., Pérez, T., Ribes, M., Romano, J.C., Serrano, E., Teixido, N., Torrents, O., Zabala, M., Zuberer, F., Cerrano, C., 2009. Mass mortality in Northwestern Mediterranean rocky benthic communities: effects of the 2003 heat wave. Global Change Biol. 15, 1090–1103, http://dx.doi.org/10.1111/j.1365-2486.2008.01823.x.
Gnaiger, E., 1983. Calculation of energetic and biochemical equivalents of respiratory oxygen consumption. In: Polarographic Oxygen Sensors. Aquatic and Physiological Applications, pp. 337–345.
Gori, A., Viladrich, N., Gili, J., Kotta, M., Cucio, C., Magni, L., Bramanti, L., Rossi, S., 2012. Reproductive cycle and trophic ecology in deep versus shallow populations of the Mediterranean gorgonian Eunicella singularis (Cap de Creus, northwestern Mediterranean Sea). Coral Reefs 31, 823–837, http://dx.doi.org/10.1007/s00338-012-0904-1.
Gori, A., Linares, C., Viladrich, N., Clavero, A., Orejas, C., Fiorillo, I., Ambroso, S., Gili, J.M., Rossi, S., 2013. Effects of food availability on the sexual reproduction and biochemical composition of the Mediterranean gorgonian *Paramuricea clavata*. J. Exp. Mar. Bio. Ecol. 444, 38–45, http://dx.doi.org/10.1016/j.jembe.2013.03.009.
Grillo, M.C., Goldberg, W.M., Allemand, D., 1993. Skeleton and sclerite formation in the precious red coral Corallium rubrum. Mar. Biol. 117, 119–128.
Guan, Y., Hohn, S., Merico, A., 2015. Suitable environmental ranges for potential coral reef habitats in the tropical ocean. PLoS One 10, e0128831, http://dx.doi.org/10.1371/journal.pone.0128831.
Guizen, K., Bramanti, L., 2014. Modelling ecological complexity for marine species conservation: the effect of variable connectivity on species spatial distribution and age structure. Theor. Biol. Forum 107, 47–56.
Heitzer, A., Kohler, H.P.E., Reichert, P., Hamer, G., 1991. Utility of phenomenological models for describing temperature dependence of bacterial growth. Appl. Environ. Microbiol. 57, 2656–2665.
Hilbish, T.J., 1986. Growth trajectories of shell and soft tissue in bivalves: seasonal variation in Mytilus edulis L. J. Exp. Mar. Bio. Ecol. 96, 103–113, http://dx.doi.org/10.1016/0022-0981(86)90236-4.
Hohn, S., Merico, A., 2012. Modelling coral polyp calcification in relation to ocean acidification. Biogeosciences 9, 4441–4454, http://dx.doi.org/10.5194/bg-9-4441-2012.
Hohn, S., Merico, A., 2015. Quantifying the relative importance of transcellular and paracellular ion transports to coral polyp calcification. Front. Earth Sci. 2, 37, http://dx.doi.org/10.3389/feart.2014.00037.
Hoogenboom, M.O., Connolly, S.R., 2009. Defining fundamental niche dimensions of corals: synergistic effects of colony size, light, and flow. Ecology 90, 767–780, http://dx.doi.org/10.1890/07-2010.1.
Kim, K., Lasker, H.R., 1998. Allometry of resource capture in colonial cnidarians and constraints on modular growth. Funct. Ecol. 12, 646–654.
Kooijman, S.A.L.M., 2010. Dynamic energy budget theory for metabolic organisation. In: Dynamic Energy Budget Theory for Metabolic Organisation, 3rd ed. Cambridge University Press, http://dx.doi.org/10.1017/CBO9780511805400.
Kruszyński, K.J., Kaandorp, J.A., Van Liere, R., 2007. A computational method for quantifying morphological variation in scleractinian corals. Coral Reefs 26, 831–840, http://dx.doi.org/10.1007/s00338-007-0270-6.
Lartaud, F., Galli, G., Raza, A., Priori, C., Benedetti, M.C., Cau, A., Santangelo, G., Iannelli, M., Solidoro, C., Bramanti, L., 2017. Growth patterns in long-lived coral species. In: Rossi, S., Bramanti, L., Gori, A., Orejas, C. (Eds.), Marine Animal Forest, The Ecology of Benthic Biodiversity Hotspots. Springer International Publishing, Switzerland.
Maltby, L., 1999. Studying stress: the importance of organism-level responses. Ecol. Appl. 9, 431–440, http://dx.doi.org/10.1890/1051-0761(1999)009[0431:SSTIOO]2.0.CO;2.
Marschal, C., Garrabou, J., Harmelin, J.G., Pichon, M., 2004. A new method for measuring growth and age in the precious red coral Corallium rubrum (L.). Coral Reefs 23, 423–432, http://dx.doi.org/10.1007/s00338-004-0398-6.
Martin, Y., Bonnefont, J.L., Chancerelle, L., 2002. Gorgonians mass mortality during the 1999 late summer in French Mediterranean coastal waters: the bacterial hypothesis. Water Res. 36, 779–782, http://dx.doi.org/10.1016/S0043-1354(01)00251-2.
McCulloch, M., Falter, J., Trotter, J., Montagna, P., 2012. Coral resilience to ocean acidification and global warming through pH up-regulation. Nat. Clim. 2, 623–627, http://dx.doi.org/10.1038/nclimate1473.
Merks, R., Hoekstra, A., Kaandorp, J., Sloot, P., 2003. Models of coral growth: spontaneous branching, compactification and the Laplacian growth assumption. J. Theor. Biol. 224, 153–166, http://dx.doi.org/10.1016/S0022-5193(03)00140-1.
Nakamura, T., Nadaoka, K., Watanabe, A., 2013. A coral polyp model of photosynthesis, respiration and calcification incorporating a transcellular ion transport mechanism. Coral Reefs 32, 779–794, http://dx.doi.org/10.1007/s00338-013-1032-2.
Neat, F.C., Wright, P.J., Fryer, R.J., 2008. Temperature effects on otolith pattern formation in Atlantic cod Gadus morhua. J. Fish Biol. 73, 2527–2541, http://dx.doi.org/10.1111/j.1095-8649.2008.02107.x.
Palmer, A.R., 1992. Calcification in marine molluscs: how costly is it? Proc. Natl. Acad. Sci. U. S. A. 89, 1379–1382, http://dx.doi.org/10.1073/pnas.89.4.1379.
Pecquerie, L., Fablet, R., De Pontual, H., Bonhommeau, S., Alunno-Bruscia, M., Petitgas, P., Kooijman, S.A.L.M., 2012. Reconstructing individual food and growth histories from biogenic carbonates. Mar. Ecol. Prog. Ser. 447, 151–164, http://dx.doi.org/10.3354/meps09492.
Picciano, M., Ferrier-Pagès, C., 2007. Ingestion of pico- and nanoplankton by the Mediterranean red coral Corallium rubrum. Mar. Biol. 150, 773–782, http://dx.doi.org/10.1007/s00227-006-0415-0.
Porter, J.W., 1976. Autotrophy, heterotrophy, and resource partitioning in Caribbean reef-building corals. Am. Nat. 110, 731–742.
Previati, M., Scinto, A., Cerrano, C., Osinga, R., 2010. Oxygen consumption in Mediterranean octocorals under different temperatures. J. Exp. Mar. Bio. Ecol. 390, 39–48, http://dx.doi.org/10.1016/j.jembe.2010.04.025.
Price, L.L., Narchi, N.E., 2015. Ethnobiology of Corallium rubrum: protection, healing, medicine, and magic. In: Narchi, N., Price, L.L. (Eds.), Ethnobiology of Corals and Coral Reefs. Springer International Publishing, Switzerland, pp. 73–86.
Priori, C., Mastascusa, V., Erra, F., Angiolillo, M., Canese, S., Santangelo, G., 2013. Demography of deep-dwelling red coral populations: age and reproductive structure of a highly valued marine species. Estuar. Coast. Shelf Sci. 118, 43–49, http://dx.doi.org/10.1016/j.ecss.2012.12.011.
Rodolfo-Metalpa, R., Martin, S., Ferrier-Pages, C., Gattuso, J.-P., 2010. Response of the temperate coral Cladocora caespitosa to mid- and long-term exposure to p CO 2 and temperature levels projected for the year 2100 AD. Biogeosciences 7, 289–300.
Rossi, S., Gili, J., 2005. Composition and temporal variation of the near-bottom seston in a Mediterranean coastal area. Estuar. Coast. Shelf Sci. 65, 385–395, http://dx.doi.org/10.1016/j.ecss.2005.05.024.
Rossi, S., Gili, J.M., 2009. Near bottom phytoplankton and seston: importance in the pelagic-benthic coupling processes. In: Kersey, W.T., Munger, S.P. (Eds.), Marine Phytoplankton. Nova Science Publishers, pp. 45–85.
Rossi, S., Tsounis, G., 2007. Temporal and spatial variation in protein, carbohydrate, and lipid levels in Corallium rubrum (Anthozoa, Octocorallia). Mar. Biol. 152, 429–439, http://dx.doi.org/10.1007/s00227-007-0702-4.
Rossi, S., Gili, J.M., Coma, R., Linares, C., Gori, A., Vert, N., 2006. Temporal variation in protein, carbohydrate, and lipid concentrations in Paramuricea clavata (Anthozoa, Octocorallia): evidence for summer-autumn feeding constraints. Mar. Biol. 149, 643–651, http://dx.doi.org/10.1007/s00227-005-0229-5.
Rossi, S., Tsounis, G., Orejas, C., Padrón, T., Gili, J.M., Bramanti, L., Teixidó, N., Gutt, J., 2008. Survey of deep-dwelling red coral (Corallium rubrum) populations at Cap de Creus (NW Mediterranean). Mar. Biol. 154, 533–545, http://dx.doi.org/10.1007/s00227-008-0947-6.
Santangelo, G., Bramanti, L., 2010. Quantifying the decline in Corallium rubrum populations. Mar. Ecol. Prog. Ser. 418, 295–297, http://dx.doi.org/10.3354/meps08898.
Santangelo, G., Carletti, E., Maggi, E., Bramanti, L., 2003. Reproduction and population sexual structure of the overexploited Mediterranean red coral Corallium rubrum. Mar. Ecol. Prog. Ser. 248, 99–108.
Santangelo, G., Bramanti, L., Iannelli, M., 2007. Population dynamics and conservation biology of the over-exploited Mediterranean red coral. J. Theor. Biol. 244, 416–423, http://dx.doi.org/10.1016/j.jtbi.2006.08.027.
Santangelo, G., Cupido, R., Cocito, S., Bramanti, L., Tsounis, G., Iannelli, M., 2012. Demography of long-lived octocorals: survival and local extinction. Proc. 12th Int. Coral Reef Symp., p9–13.
Sebens, K.P., 1980. The regulation of asexual reproduction and indeterminate body size in the sea anemone Anthopleura elegantissima (Brandt). Biol. Bull. 158, 370–382.
Sebens, K.P., 1987. The ecology of indeterminate growth in animals. Annu. Rev. Ecol. Syst. 18, 371–407.
Sebens, K.P., 2002. Energetic constraints, size gradients, and size limits in benthic marine invertebrates. Integr. Comp. Biol. 42, 853–861, http://dx.doi.org/10.1093/icb/42.4.853.
Solidoro, C., Pastres, R., Melaku Canu, D., Pellizzato, M., Rossi, R., 2000. Modeling the growth of Tapes philippinarum in Northern Adriatic lagoons. Mar. Ecol. Prog. Ser. 199, 137–148.
Solidoro, C., Melaku Canu, D., Rossi, R., 2003. Ecological and economic considerations on fishing and rearing of Tapes phillipinarum in the lagoon of Venice. Ecol. Model. 170, 303–318, http://dx.doi.org/10.1016/S0304-3800(03)00235-7.
Tambutté, S., Tambutté, E., Zoccola, D. and Allemand, D. (2007) Organic Matrix and Biomineralization of Scleractinian Corals, in Handbook of Biomineralization: Biological Aspects and Structure Formation (ed E. Bäuerlein), Wiley-VCH Verlag GmbH, Weinheim, Germany. doi: 10.1002/9783527619443.ch14.
Tsounis, G., Rossi, S., Aranguren, M., Gili, J.M., Arntz, W., 2006a. Effects of spatial variability and colony size on the reproductive output and gonadal development cycle of the Mediterranean red coral (Corallium rubrum L.). Mar. Biol. 148, 513–527, http://dx.doi.org/10.1007/s00227-005-0100-8.
Tsounis, G., Rossi, S., Laudien, J., Bramanti, L., Fernández, N., Gili, J.M., Arntz, W., 2006b. Diet and seasonal prey capture rates in the Mediterranean red coral (Corallium rubrum L.). Mar. Biol. 149, 313–325, http://dx.doi.org/10.1007/s00227-005-0220-1.

Tsounis, G., Rossi, S., Gili, J.M., Arntz, W., 2007. Red coral fishery at the costa brava (NW mediterranean): case study of an overharvested precious coral. Ecosystems 10, 975–986.
Tsounis, G., Rossi, S., Grigg, R., Santangelo, G., Bramanti, L., Gili, J.-M., 2010. The exploitation and conservation of precious corals. Oceanography and Marine Biology. Ann. Rev. 48, 161–212.
Ursin, E., 1967. A mathematical model of some aspects of fish growth, respiration and mortality. J. Fish. Res. Board Can. 24, 2355–2453.
von Bertalanffy, L., 1938. A quantitative theory of organic growth (inquiries on growth laws. II). Hum. Biol. 10, 181–213.
Weinbauer, M.G., Brandstätter, F., Velimirov, B., 2000. On the potential use of magnesium and strontium concentrations as ecological indicators in the calcite skeleton of the red coral (Corallium rubrum). Mar. Biol. 137, 801–809, http://dx.doi.org/10.1007/s002270000432.
Zibrowius, H., Monteiro Marques, V., Grasshoff, M., 1984. La répartition du corallium rubrum dans lAtlantique (Cnidaria: Anthozoa: Gorgonaria). Tethys 11, 163–170.